Surface & Coatings Technology 331 (2017) 15–20

Contents lists available at ScienceDirect

Surface & Coatings Technology

journal homepage: www.elsevier.com/locate/surfcoat

Improved interfacial adhesion between TiAlN/DLC multi-layered coatings by controlling the morphology via bias

Liangliang Liu[a], Zhongzhen Wu[a,b,*], Xiaokai An[a], Tielei Shao[a], Shu Xiao[a], Suihan Cui[a], Hai Lin[a], Ricky K.Y. Fu[b], Xiubo Tian[a], Paul K. Chu[b], Feng Pan[a,**]

[a] School of Advanced Materials, Peking University Shenzhen Graduate School, Shenzhen 518055, China
[b] Department of Physics and Materials Science, City University of Hong Kong, Tat Chee Avenue, Kowloon, Hong Kong, China

ARTICLE INFO

Keywords:
TiAlN/DLC
Interfacial adhesion
Morphology
Substrate bias

ABSTRACT

By combining the advantages of the thermo-mechanical properties of TiAlN and self-lubricating properties of diamond-like carbon (DLC), a multi-layered TiAlN/DLC coating is fabricated by filtered cathodic vacuum arc and magnetron sputtering. According to the different morphology and mismatch between the physical and chemical properties of TiAlN and DLC, multiple methods are used to study the growth mechanism of crystalline TiAlN and amorphous DLC in the combined system. The morphology evolution depending on the bias is studied and the brittle interface is assessed by scratch experiments. The results show that an interlamination failure occurs at the top of first DLC layer due to the cluster morphology obtained by small bias, however, the failure moves to the interface above the substrate when the clusters are refined by increasing bias. By adopting the stepwise decreased bias, the 4.5 μm thick TiAlN/DLC multi-layer coating is fabricated and does not exhibit interfacial failure at any interface between TiAlN and DLC in the scratch experiments up to a load of 100 N. Excellent adhesion (Lc = 63 N) is also achieved from coatings deposited on high-speed steel with optimized Cr/CrCx/CrC interlayers prepared by high-power impulse magnetron sputtering.

1. Introduction

Owing to the excellent mechanical properties and thermal stability, TiAlN coatings are commonly applied as protective layers to cutting and forming tools as well as other applications [1–3]. However, the friction coefficient of TiAlN, especially under dry conditions, is quite large reaching 0.9–1.0 at room temperature and 1.5 at 400 °C [4]. Diamond-like carbon (DLC) coatings, especially hydrogenated DLC coatings (a-C:H), are known for their excellent tribological properties such as small friction coefficients (0.05–0.2) and wear rates ($< 10^{-15}$ m^3/N·m) [5,6]. However, the hardness of a-C:H films are typically < 20 GPa which is smaller than that of TiAlN or TiAlSiN.

Multi-layered coatings with alternating and different compositions can combine the advantages of the constituent layers and are preferred to enhance integrated performance over single-layered coatings [7–9]. Both hard and self-lubricating multi-layered coatings are expected to prepared by choosing the proper combinations, for example, multi-layered TiAlN/VN, TiAlN/WC, TiAlN/MoN, and so on [10–12]. However, although the wear resistance can be improved and friction can be reduced, the self-lubrication effects of these coatings are still worse than that of a-C:H. However, when a-C:H coatings are used to construct a multi-layered structure with TiAlN, problems occur. For instance, it is difficult to prepare amorphous DLC on crystalline TiAlN and vice versa due to the mismatch between the physical and chemical properties of the two materials and film adhesion is also an issue in the system combining TiAlN and DLC [13,14].

In this study, TiAlN/DLC multi-layered coatings are prepared by filtered cathodic vacuum arc (FCVA) and magnetron sputtering and the growth mechanism of the crystalline TiAlN and amorphous DLC layers on each other are studied. The brittle interface is assessed by scratch experiments and the adhesion mechanism is investigated by controlling the morphology and stress. By adopting the suitable bias and composition, the 4.5 μm thick TiAlN/DLC multi-layered coating is fabricated without failure happening at any interface between TiAlN and DLC and an adhesion strength of 63 N is achieved with optimized Cr/CrC interlayers fabricated by high-power impulse magnetron sputtering (HiPIMS).

* Correspondence to: Z. Wu, School of Advanced Materials, Peking University Shenzhen Graduate School, Shenzhen 518055, China.
** Corresponding author.
E-mail addresses: wuzz@pkusz.edu.cn (Z. Wu), Panfeng@pkusz.edu.cn (F. Pan).

http://dx.doi.org/10.1016/j.surfcoat.2017.10.029
Received 13 July 2017; Received in revised form 22 September 2017; Accepted 8 October 2017
Available online 09 October 2017
0257-8972/

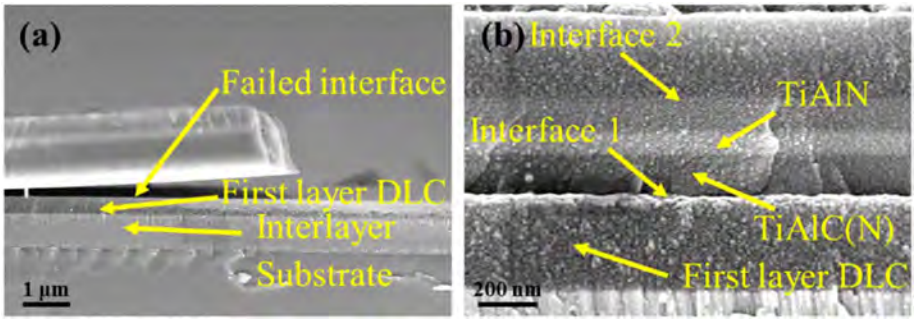

Fig. 1. Cross-sectional images of the TiAlN/DLC multi-layered coating: (a) fragile position, (b) interfaces between DLC and TiAlN (Interface 1) and between TiAlN and DLC (Interface 2).

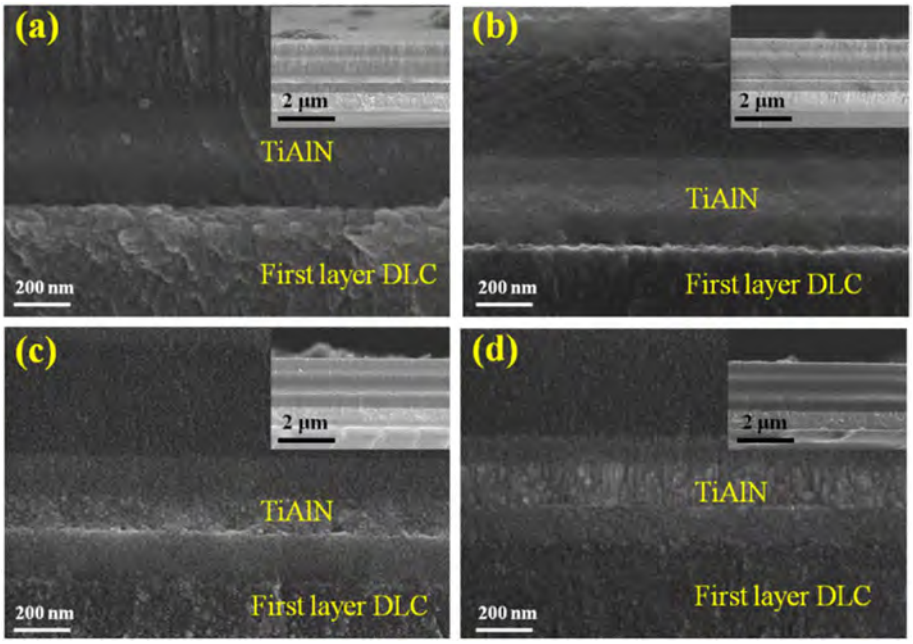

Fig. 2. Cross-sectional images of the TiAlN/DLC multi-layered coatings prepared at different biases: (a) − 50 V, (b) − 100 V, (c) − 150 V, and (d) − 150 V.

2. Experimental details

A multi-functional plasma surface modification and coating deposition system designed by our lab with a vacuum chamber (diameter of 100 cm and height of 80 cm) was used for the deposition at 200 °C and a base pressure of 8×10^{-4} Pa. High-speed steel (HSS) and single-crystal silicon (100) samples were used as substrates. The target-substrate distance was fixed at 14 cm in the experiment. The HSS substrates ($\Phi 25 \times 4$ mm) were polished with abrasive SiC paper from 320 to 1500 grits and then up to 1 μm with diamond paste with a velvet cloth manually. All the substrates were ultrasonically cleaned for 30 min in alcohol, acetone, and deionized water sequentially and dried at 120 °C. Before deposition, the substrates were further cleaned for 20 min with an Ar plasma (40 sccm, 0.8 Pa) using an anode layer ion source (Cehis 100, Plasma Technology Ltd. Hong Kong) at a power of 300 W and bias of − 500 V in the deposition chamber. To enhance film adhesion, an optimized Cr/CrC_x/CrC interlayer was produced under Ar (99.999% pure) and C_2H_2 (99.8% pure) using a 530 × 100 mm Cr target (99.99% pure) by HiPIMS with pulses voltage of 750 V, frequency of 50 Hz, pulse width of 300 μs (SIPP 2000, Melec GmbH, Germany). The DLC film was fabricated using a 530 × 100 mm C target (99.99% pure) under the same conditions with a DC power of 2400 W (480 V, 5 A) (SIPP 2000 Melec GmbH, Germany). To obtain a gradient transition of C at the interface between the DLC and TiAlN layers, the on/off flow of C_2H_2 and N_2 (C_2H_2 flow changed from 40 sccm to 0 sccm while N_2 flow from 0 sccm to 15 sccm and vice versa before DLC deposition) was controlled carefully and slowly when the TiAlN layer was deposited by 90° curved magnetic FCVA (FCVA133, Plasma Technology Ltd. Hong Kong) using a $Ti_{70}Al_{30}$ target ($\Phi 71 \times 50$ mm, 99.99% pure) in the presence of a carrier gas (Ar) and reactive gas (N_2). The arc voltage and current were 35 V and 60 A, respectively, and a 10 A current was applied to the coil to produce the extraction magnetron.

The morphology was observed by field-emission scanning electron microscopy (FE-SEM, ZEISS SUPRA® 55) equipped with an energy-dispersive X-ray spectrometer (EDS), atomic force microscopy (AFM, Bruker multimode 8) and transmission electron microscopy (TEM, JEM-3200FS) equipped with an energy-dispersive X-ray spectrometer (Thermo UltraDry, America). A scratch test instrument (WS-2005, Zhongke Kaihua Technology, China) equipped with acoustic emission was employed in the scratch test to evaluate the adhesion strength between the films and substrate. Normal loads were applied progressively from 0 N to 100 N for 3 mm/min at a sliding rate of 50 N/min. The scratch tracks and depths were examined by 3D laser confocal microscopy (KEYENCE, VK-× 200) and the results were verified by EDS.

3. Result and discussion

In order to enhance the adhesion strength between the coating and substrate, a gradient Cr/CrC_x/CrC interlayer is introduced to reduce the mismatch in thermal expansivity and element compositions. To obtain a gradient transition of C at the interface between the DLC and TiAlN layer, the C_2H_2 and N_2 flow rates are controlled carefully and gradually during deposition of the TiAlN layer. The C_2H_2 flow rates are changed from 40 sccm to 0 sccm while that of N_2 are rising from 0 sccm to 15 sccm gradually at the same time and vice versa before DLC

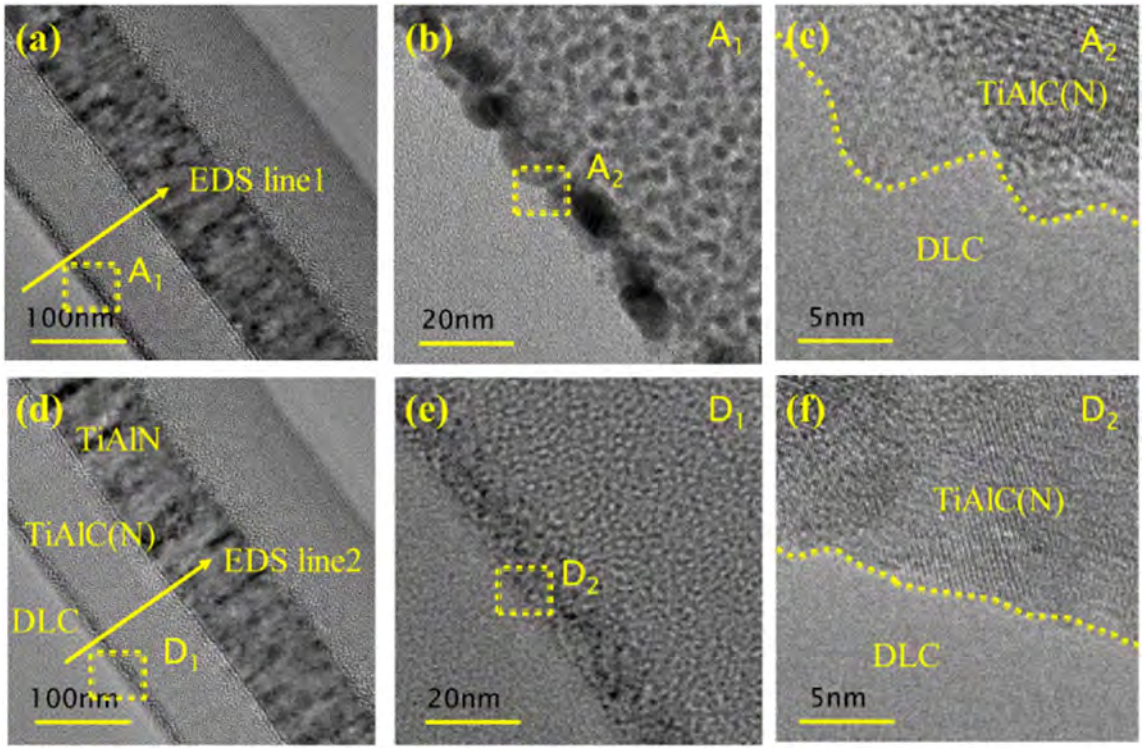

Fig. 3. TEM cross-sectional images of the interface between the first DLC layer and TiAlN layer fabricated at (a) − 50 V; (b–c) magnified images of A1, A2 in (a); (d) − 200 V; (e–f) magnified images of D1, D2 in (d).

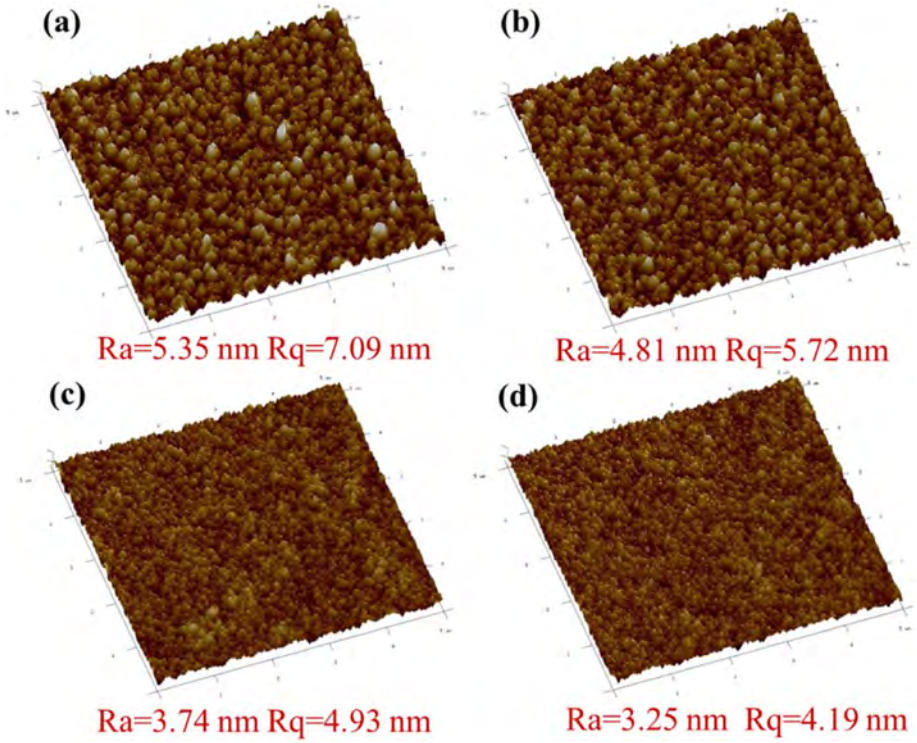

Fig. 4. Surface morphology of the first DLC layers prepared at different biases examined by AFM: (a) − 50 V, (b) − 100 V, (c) − 150 V, and (d) − 200 V.

deposition. However, the adhesion was poor. Fig. 1 shows the cross-sectional morphology of the failed interface in the TiAlN/DLC multi-layered coating and the magnified images of the coatings that did not peel off. Failure always occurs at the interface between the first DLC layer and the next TiAlC(N) layer (Interface 1 in Fig.1(b)) although the transition processes at each TiAlC(N)/DLC and DLC/TiAlC(N) interface are the same (as shown in Fig. 1(a)). Fig.1(b) gives the enlarged view of the coatings that did not peel off. Further study of the morphology of each layer reveals that growth of the first DLC layer is more distinct than that of the other DLC layers and adhesion between the first DLC layer and the next TiAlN layer is weaker, as shown in Fig. 1(b). The first DLC layer shows an apparent clustery and rough structure which is different from the fine and smooth morphology observed from the TiAlC(N) layer. The cluster size decreases in the subsequent DLC layers

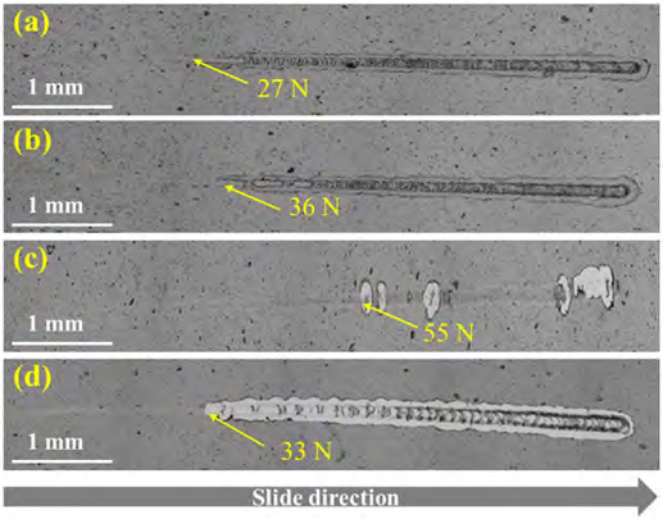

Fig. 5. Scratch morphology of the TiAlN/DLC multi-layered coatings prepared at different biases: (a) − 50 V, (b) − 100 V, (c) − 150 V, and (d) − 200 V.

similar to TiAlC(N) and this may explain the better adhesion at the other interfaces. Considering the large columnar grain structure of the Cr/CrC_x/CrC interlayer under the first DLC layer, the large DLC cluster formed during "coping profile" growth along the large columnar CrC grains in the interlayer may determine the morphology of the first DLC layer. However, the TiAlC(N) layer always shows a fine grain structure and the morphological difference may contribute to the adhesion.

The sample bias has been reported to change the morphology of DLC coatings, that is, from large grains or clusters to small ones with increasing ion energy [15]. Hence, four samples were fabricated at different biases in our experiments to control the morphology of the first DLC layer and the results are shown in Fig. 2. The TiAlN/DLC bi-layer is repeated 2.5 times for each samples to achieve an overall coating thickness of 3 μm including the Cr/CrCx/CrC interlayer with a thickness of about 1 μm. The thickness of each DLC layer is 400 nm and the TiAlN layer possesses a sandwich structure with a 140 nm thick TiAlN film infibulated by two 130 nm graded transition layers (from TiAlC to TiAlN or TiAlN to TiAlC) on each side because of the varying deposition atmosphere to improve adhesion with the DLC layer. As expected, the large clusters in first DLC layer shown in Fig. 2(a) change to a fine and smooth morphology when the bias is changed from − 50 V to − 200 V. At the same time, the TiAlN layers retain the fine and smooth structure regardless of bias [16,17] and the interface between the first DLC layer and the next TiAlN layer is smooth and continuous without defects at high bias indicating an good adhesion as shown in Figs. 2(a) to 2(d).

In order to confirm the detailed chemical transition at the interface between the first DLC layer and TiAlN, the TEM and EDS are performed and the results are shown in Fig. 3. For comparison, two samples prepared with the bias of − 50 V and − 200 V are selected. The TEM results show that the interface between the first DLC layer and TiAlC(N) is bumpy and depends on the DLC morphology when the bias is − 50 V, however, it becomes smooth and flat when the bias increases to − 200 V due to the refined DLC particles. The chemical transitions (without been given in the article due to the little difference) are similar with the transition zone of about 20 nm from DLC to TiAlC(N) whatever the bias is because of the same deposition parameters of the follow layer.

To monitor the morphology evolution of the first DLC layer, samples with only the first DLC layer are prepared at different biases and the AFM images are depicted in Fig. 4. The sample prepared at − 50 V has a roughness of Ra = 5.35 nm (Rq = 7.09 nm) due to the presence of clusters with a diameter of about 300 nm. With increasing bias, both the cluster size and surface roughness decrease. This phenomenon is more obvious compared to the samples deposited at − 150 V (Ra = 3.74 nm, Rq = 4.93 nm) and − 200 V (Ra = 3.25 nm, Rq = 4.19 nm) which are relatively flat. As the sample bias is increased, the C ion energy goes up and C mobility is enhanced [18,19] giving rise to reduced surface roughness and cluster size [20].

The scratch morphology of the TiAlN/DLC multi-layered coatings formed at different biases is presented in Fig. 5. The scratch is obtained by applying a progressively increasing normal load from 0 to 100 N at a sliding speed of 3 mm/min and loading speed of 50 N/min. Five scratches are performed for each sample and no significant difference is obtained. The one presented in this work has the critical load value closest to the average value. The four samples show critical loads of

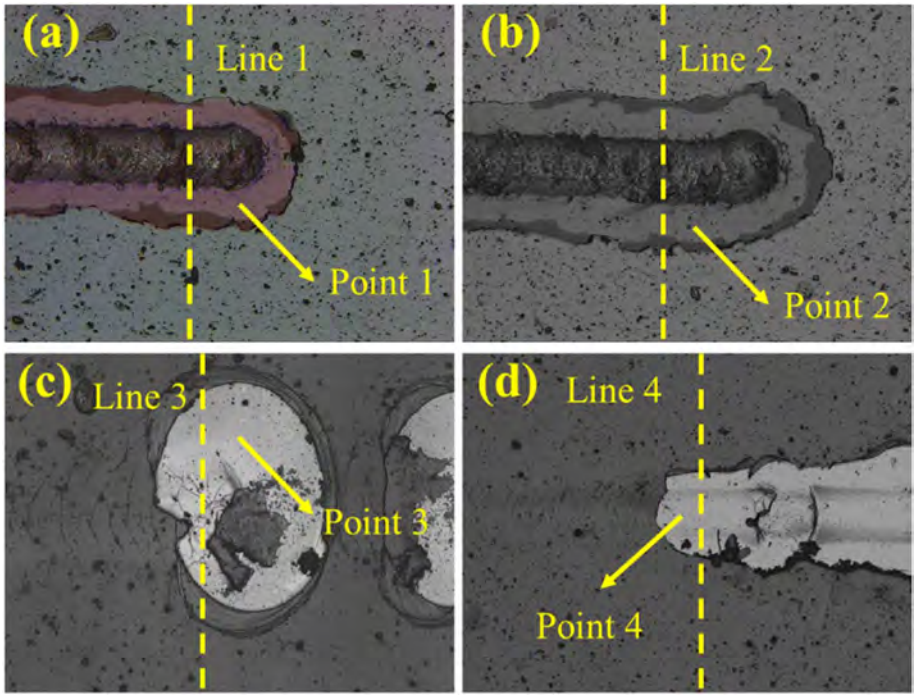

Fig. 6. Magnified morphology of the representative scratch positions of the TiAlN/DLC multi-layer coatings prepared at different biases: (a) − 50 V, (b) − 100 V, (c) − 150 V, and (d) − 200 V.

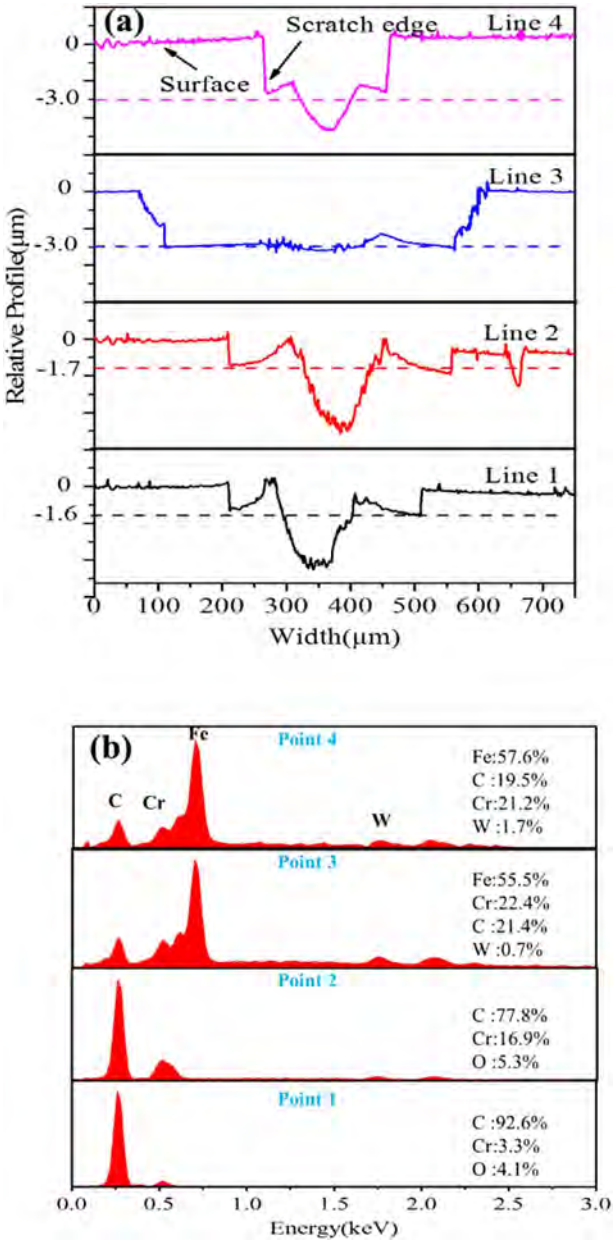

Fig. 7. (a) 3 D profiles of lines 1, 2, 3, and 4 and (b) Element composition of points 1, 2, 3, and 4 in Fig. 6.

27 N, 36 N, 55 N, and 33 N, respectively, based on when breakage first occurs, indicating improved adhesion initially with increasing bias and decreased adhesion when the bias is larger than − 150 V. There are differences in the morphology of the failed regions as shown in Figs. 5(a)–5(d). As shown in Figs. 5(a) and 5(b), delamination occurs at the edge of the scratch. Although delamination continues to the end, no obvious exposed substrate can be observed from the failed locations, indicating poor adhesion at some interlamination interfaces which is even worse than that between the coating and substrate. When the bias is larger than − 150 V, the coating shows peeling and the silvery surface seen at the failed locations is likely that of the HHS substrate or Cr/CrC interlayer, indicating the interlamination adhesion is enhanced. When the bias is − 200 V, significant cracking and flaking occur at a critical load of 33 N.

To determine the locations of failure on each sample, profiles are acquired by 3D confocal microscopy as shown in Fig. 6. The depth information along lines 1, 2, 3, and 4 in Fig. 6 and elemental composition at points 1, 2, 3 and 4 determined by EDS are presented in Fig. 7. The height of the step between the coating surface and flakes for lines 1 and 2 is about 1.6 μm, indicating that the fragile position is the interface between the first DLC layer and next TiAlN layer consistent with SEM (Fig. 2). However, the height of the step for lines 3 and 4 is about 3 μm corresponding to the thickness of the whole coating, indicating that failure occurs at the interface between the Cr interlayer and HSS substrate. The same conclusion can be drawn based on the composition at the scratch in Fig. 7. The main element at points 1 and 2 is carbon whereas points 3 and 4 show mainly iron. According to film growth theory, a smooth surface is suitable for ion migration and diffusion for adhesion improvement [21,22]. Owing to the rough surface of the first DLC layer, the coating peels off at this interface. As shown in Figs. 2, 3 and 4, the cluster size of the first DLC layer decreases with increasing bias resulting in improved adhesion at the interlamination interfaces. However, although the film morphology can be adjusted with the bias, the bias also affects the properties of TiAlN and DLC, especially the internal stress which can influence adhesion of multi-layered coatings [23,24]. Therefore, when the bias exceeds 150 V, adhesion becomes poor again as manifested by structural failure of all the layers.

As aforementioned, the morphology mismatch between the DLC clusters and TiAlN layer occurs at the interface above the first DLC layer and induces interlamination failure. In comparison, no failure is observed at the other interfaces. Failure at the interface above the substrate may be attributed to the stress accumulated until the end of deposition. Hence, gradually decreasing biases are applied during deposition. A − 150V bias is used for the first DLC and TiAlN layer (first modulation period) and is decreased by 10 V each during subsequent modulation periods. Finally, a 4.5 μm thick TiAlN/DLC multi-layered coatings is fabricated and the cross-sectional SEM images are shown in Fig. 8. As expected, the morphology of the first DLC layer is refined and smoothed and matches the TiAlN layer well. The transition is smooth and continuous at all the interfaces thus giving rise to excellent interfacial adhesion. The scratch morphology in Fig. 9(a) confirms excellent adhesion with a value of 63 N. The 3D profile of line 5 and composition of point 5 in Fig. 9(a) are shown in Figs. 9(b) and 9(c). The step height between the coating surface and failed position is about 4.5 μm

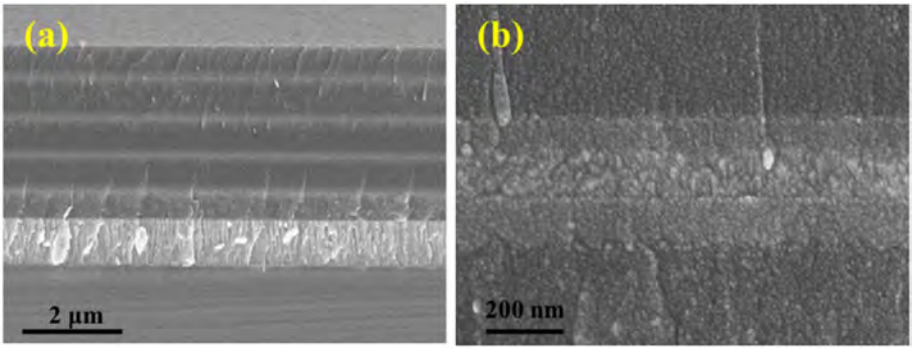

Fig. 8. Cross-sectional images of the TiAlN/DLC multi-layered coating prepared with stepwise decreasing bias: (a) Whole view of the cross-section and (b) Morphology of the TiAlN/DLC interface.

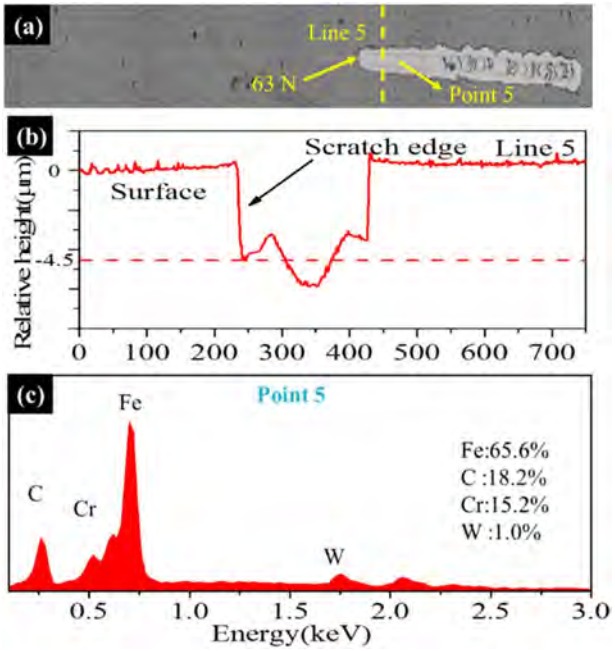

Fig. 9. Scratch result of the TiAlN/DLC multi-layered coating prepared with stepwise decreasing bias: (a) Scratch morphology, (b) 3D profile of line 5, and (c) Elemental composition of point 5.

corresponding to the coating thickness and the composition exposed is confirmed to be HSS. These results suggest that failure occurs at the substrate-interlayer-interface and not through delamination in between the functional DLC/TiAlN multilayers.

4. Conclusion

In an attempt to obtain hard and self-lubricating coatings, TiAlN/DLC multilayers are fabricated by FCVA and magnetron sputtering. The growth and adhesion mechanisms of the amorphous DLC layer and crystalline TiAlN layer are studied. When the bias is small, “coping profile” growth plays an important role in the DLC layers but when the bias is increased, the high atomic mobility and nucleation rate as a result of the larger ion energy refine and smooth the DLC clusters. The morphology of TiAlN layer is found to be independent of the bias and it always shows a fine and smooth structure. Adhesion failure occurs at the interlamination interface for small biases and commences at the interface above the substrate for large biases. A 4.5 μm thick TiAlN/DLC multi-layered coating with excellent adhesion (Lc = 63 N) is obtained by means of stepwise decreasing bias in order to accommodate the growth morphology and internal stress.

Acknowledgements

This work was financially jointly supported by Shenzhen Science and Technology Research Grants (JCYJ20150828093127698 and JCYJ20170306165240649), as well as City University of Hong Kong Applied Research Grant (ARG) No. 9667122 and Strategic Research Grant (SRG) No. 7004644.

References

[1] N. Norrby, M.P. Johansson-Jõesaar, M. Odén, Improved metal cutting performance with bias-modulated textured $Ti_{0.50}Al_{0.50}N$ multilayers, Surf. Coat. Technol. 257 (2014) 102–107.
[2] P.H. Mayrhofer, A. Hörling, L. Karlsson, J. Sjölén, T. Larsson, C. Mitterer, L. Hultman, Self-organized nanostructures in the Ti–Al–N system, Appl. Phys. Lett. 83 (2003) 2049–2051.
[3] W.D. Münz, Titanium aluminum nitride films: a new alternative to TiN coatings, J. Vac. Sci. Technol. A 4 (1986) 2717–2725.
[4] J. Hardell, B. Prakash, Tribological performance of surface engineered tool steel at elevated temperatures, Int. J. Refract. Met. Hard Mater. 28 (2010) 106–114.
[5] J. Robertson, Diamond-like amorphous carbon, Mater. Sci. Eng. R 37 (2002) 129–281.
[6] H.S. Zhang, J.L. Endrino, A. Anders, Comparative surface and nano-tribological characteristics of nanocomposite diamond-like carbon thin films doped by silver, Appl. Surf. Sci. 255 (2008) 2551–2556.
[7] J.S. Koehler, Attempt to design a strong solid, Phys. Rev. B: Condens. Matter 2 (1970) 547–551.
[8] Y. Hu, L. Li, X. Cai, Q. Chen, P.K. Chu, Mechanical and tribological properties of TiC/amorphous hydrogenated carbon composite coatings fabricated by DC magnetron sputtering with and without sample bias, Diam. Relat. Mater. 16 (2007) 181–186.
[9] M.X. Wang, J.J. Zhang, J. Yang, L.Q. Wang, D.J. Li, Influence of Ar/N_2 flow ratio on structure and properties of nanoscale ZrN/WN multilayered coatings, Surf. Coat. Technol. 201 (2007) 5472–5476.
[10] V. Derflinger, H. Brändle, H. Zimmermann, New hard/lubricant coating for dry machining, Surf. Coat. Technol. 113 (1999) 286–292.
[11] P.E. Hovsepian, Q. Luo, G. Robinson, M. Pittman, M. Howarth, D. Doerwald, R. Tietema, W.M. Sim, A. Deeming, T. Zeus, TiAlN/VN superlattice structured PVD coatings: a new alternative in machining of aluminium alloys for aerospace and automotive components, Surf. Coat. Technol. 201 (2006) 265–272.
[12] A. Biksa, K. Yamamoto, G. Dosbaeva, S.C. Veldhuis, G.S. Fox-Rabinovich, A. Elfizy, T. Wagg, L.S. Shuster, Wear behavior of adaptive nano-multilayered AlTiN/MexN PVD coatings during machining of aerospace alloys, Tribol. Int. 43 (2010) 1491–1499.
[13] Y. Liu, I. Bhamji, P.J. Withers, D.E. Wolfe, A.T. Motta, M. Preuss, Evaluation of the interfacial shear strength and residual stress of TiAlN coating on ZIRLO™ fuel cladding using a modified shear-lag model approach, J. Nucl. Mater. 466 (2015) 718–727.
[14] S. Zhang, H.T. Johnson, G.J. Wagner, W.K. Liu, K.J. Hsia, Stress generation mechanisms in carbon thin films grown by ion-beam deposition, Acta Mater. 51 (2003) 5211–5222.
[15] A. Saeheng, N. Tonanon, W. Bhanthumnavin, B. Paosawatyanyong, Sulphur doped DLC films deposited by DC magnetron sputtering, Can. J. Chem. Eng. 90 (2012) 909–914.
[16] G.S. Fox-Rabinovich, G.C. Weatherly, A.I. Dodonov, A.I. Kovalev, L.S. Shuster, S.C. Veldhuis, G.K. Dosbaeva, D.L. Wainstein, M.S. Migranov, Nano-crystalline filtered arc deposited (FAD) TiAlN PVD coatings for high-speed machining applications, Surf. Coat. Technol. s 177–178 (2004) 800–811.
[17] N. Mustapha, R.P. Howson, Optical TiN films by filtered arc evaporation, Surf. Coat. Technol. 92 (1997) 29–33.
[18] Y. Wang, Y. Ye, H. Li, J. Li, J. Chen, H. Zhou, A magnetron sputtering technique to prepare a-C:H films: effect of substrate bias, Appl. Surf. Sci. 257 (2011) 1990–1995.
[19] N. Ravi, V.L. Bukhovets, I.G. Varshavskaya, G. Sundararajan, Deposition of diamond-like carbon films on aluminium substrates by RF-PECVD technique: influence of process parameters, Diam. Relat. Mater. 16 (2007) 90–97.
[20] I. Petrov, P.B. Barna, L. Hultman, J.E. Greene, Microstructural evolution during film growth, J. Vac. Sci. Technol. A 21 (2009) S117–S128.
[21] J. Sellers, Asymmetric bipolar pulsed DC: the enabling technology for reactive PVD, Surf. Coat. Technol. 98 (1998) 1245–1250.
[22] J.W. Lee, S.K. Tien, Y.C. Kuo, The effects of pulse frequency and substrate bias to the mechanical properties of CrN coatings deposited by pulsed DC magnetron sputtering, Thin Solid Films 494 (2006) 161–167.
[23] M. Ahlgren, H. Blomqvist, Influence of bias variation on residual stress and texture in TiAlN PVD coatings, Surf. Coat. Technol. 200 (2005) 157–160.
[24] R.K. Wang, S.P. Min, U.C. Jung, A.R. Kwon, W.K. Yong, W.S. Chung, Effect of voltage on diamond-like carbon thin film using linear ion source, Surf. Coat. Technol. 243 (2014) 15–19.